

<https://doi.org/10.1038/s43247-024-01893-8>

Ladder fuels rather than canopy volumes consistently predict wildfire severity even in extreme topographic-weather conditions

Check for updates

Christopher R. Hakkenberg ¹ ✉, Matthew L. Clark ², Tim Bailey ³, Patrick Burns ¹ & Scott J. Goetz ¹

Drivers of forest wildfire severity include fuels, topography and weather. However, because only fuels can be actively managed, quantifying their effects on severity has become an urgent research priority. Here we employed GEDI spaceborne lidar to consistently assess how pre-fire forest fuel structure affected wildfire severity across 42 California wildfires between 2019–2021. Using a spatial-hierarchical modeling framework, we found a positive concave-down relationship between GEDI-derived fuel structure and wildfire severity, marked by increasing severity with greater fuel loads until a decline in severity in the tallest and most voluminous forest canopies. Critically, indicators of canopy fuel volumes (like biomass and height) became decoupled from severity patterns in extreme topographic and weather conditions (slopes $>20^\circ$; winds >9.3 m/s). On the other hand, vertical continuity metrics like layering and ladder fuels more consistently predicted severity in extreme conditions – especially ladder fuels, where sparse understories were uniformly associated with lower severity levels. These results confirm that GEDI-derived fuel estimates can overcome limitations of optical imagery and airborne lidar for quantifying the interactive drivers of wildfire severity. Furthermore, these findings have direct implications for designing treatment interventions that target ladder fuels versus entire canopies and for delineating wildfire risk across topographic and weather conditions.

Wildfires are an essential ecosystem process that maintains forest productivity, biodiversity, function, and resilience¹. Throughout the pre-European Western US, frequent fires were a common phenomenon, including those set intentionally by Indigenous Peoples^{2,3}. However, elevated tree densities compared to the pre-industrial baseline after more than a century of intensive fire suppression as well as pervasive climate warming have contributed to wildfires of increasing size and severity^{4–6}. This trend toward historically uncharacteristic high-severity fires has resulted in wildfire regimes that are more destructive to forest ecosystems and more dangerous to human communities^{7,8}. The occurrence of larger, more severe wildfires has also had an acute effect on post-fire forest transitions. Whereas mixed-severity wildfires in fire-adapted systems may result in pyrodiverse landscape mosaics that enable multi-scale biodiversity, habitat, and

ecological resilience^{9–11}, large high-severity fires are associated with arrested long-term forest regrowth and even type conversion from forest to non-forest due to their impact on microclimate, soil conditions and seed bank viability^{12,13}.

The drivers of wildfire severity are complex and interconnected, but can be described as an interaction among three primary factors: fuels, topography and weather⁴. While fuels and topography are conceived as bottom-up forces with localized effects, weather conditions and climatic trends are top-down controls that operate at broader spatial scales^{15,16}. Ultimately, the relative influence of top-down versus bottom-up controls on fire behavior is context-dependent and contingent on chance factors¹⁴. Some studies have found the accumulation of dense fuel loads to be the most important factor driving high-severity fire^{8,17}. Other studies have found

¹School of Informatics, Computing & Cyber Systems, Northern Arizona University, Flagstaff, AZ, USA. ²Center for Interdisciplinary Geospatial Analysis, Department of Geography, Environment, & Planning, Sonoma State University, Rohnert Park, CA, USA. ³Redwood Forest Foundation, Fort Bragg, CA, USA.

✉ e-mail: chris.hakkenberg@nau.edu

climate change and weather conditions to overwhelm fuel loads to dominate fire behavior^{5,18}. However, unlike weather and climate conditions, only fuels can be actively managed; for instance via mechanical thinning or cultural burns^{2,19,20}. Therefore, quantifying the influence of forest fuel structure on fire severity has been identified as a top wildfire research priority with direct bearing on critical forest management planning and policy decisions²¹.

Research into the role of fuel structure in driving landscape patterns in burn severity has generally been restricted to 2D optical imagery (i.e. satellite-derived canopy cover), which fails to characterize the sub-canopy, or to the few instances where airborne lidar scanning (ALS) is sufficient in extent and timely in relation to wildfires²². However, ALS's limited coverage, relatively high costs and slow data delivery times, in addition to inconsistency among flight lines, sensor specifications and data products have hindered its widespread adoption for inference into generalized trends across fires, regions, and years^{23,24}. Otherwise, some researchers have employed simulations or modeled datasets on fuels, such as those from LANDFIRE, though these data lack the vertical precision and temporal cadence for application to local-scale management and specific time periods²⁵. These data limitations have greatly constrained the research community's ability to consistently assess the empirical relationship between forests fuels and burn severity across regions, as well as our ability to infer how fuels interact with weather and topography (hereafter, "topo-weather") to drive severity patterns in widely varying contexts.

In this vein, the Global Ecosystem Dynamics Investigation (GEDI) spaceborne lidar is novel for its ability to provide consistent samples of 3-dimensional fuel structure across broad spatial extents and over multiple years^{26,27}. GEDI is a waveform lidar sampling instrument installed on the International Space Station (ISS). Each GEDI waveform corresponds to a discrete 25 m diameter footprint on the Earth surface that characterizes the vertical distribution of vegetation biomass from the ground to the top of the canopy. With progressive orbital acquisitions since April 2019, the spatial coverage of these waveform samples has increased to include over 7 billion high-quality filtered footprints between 52 degrees south and north latitudes. Geographically distributed GEDI samples can be used to derive large-scale, multi-year estimates of vegetation structure that provide actionable information for estimating wildfire fuel loads previously unattainable with satellite optical imagery or piecemeal ALS datasets. While GEDI does not provide all aspects of fuel properties needed to predict wildfire behavior, such as pre-fire moisture content and foliar chemical composition, it does provide readily-applicable analogues to traditional wildfire fuel structure parameters such as canopy height, canopy bulk density (CBD) and canopy fuel load (CFL)^{28,29}.

Critical to assessing the role of fuel structure in driving wildfire severity across regions and years is a thorough accounting for how the relationship changes across topographic, weather, and climate conditions¹⁵. For example, fire weather is a dominant top-down control on burn severity, as quantified by indicators related to pre-fire vegetation water stress and fuel moisture conditions like vapor pressure deficit (VPD)³⁰ and evapotranspiration (ET)³¹. As for topography, flatter areas in mountainous terrain tend to be less sun-exposed and therefore cooler, moister, and less susceptible to fire regardless of fuel distributions, though this relationship may be reversed depending on context¹⁹. With increasing slope comes a tendency towards increasing severity, especially with uphill fire spread³², until slopes are so steep (e.g. sheer cliffs) that they function as firebreaks³³. Similarly, high winds may facilitate contagion via crown spread and ember cast⁶. Despite a relative degree of clarity on how fuels, topography and weather work in isolation to drive wildfire severity patterns from specific local case studies, far less is known about how these factors interact in varying geographic and climate contexts based on spatio-temporally consistent measurements of forest structure, previously unavailable at scale prior to GEDI³⁴.

Importantly, if topography and fire weather conditions can overwhelm fuel structure patterns – especially where that forest structure has been altered through costly management interventions – knowing the threshold values for both structural attributes and topo-weather conditions will be of critical importance to forest managers and fire science researchers. High-intensity fuel treatments (i.e. those that remove entire forest canopies)

versus those that focus on vertical continuity (especially understory thinning of ladder fuels or cultural burns) could lead to very different severity outcomes in varying topo-weather conditions³⁵. Improved clarity on the nature of these relationships can provide a deeper understanding of process and pattern in fire science, with practical applications for modeling wildfire hazard, treatment design and containment strategies^{35,36}.

In this study, we employed large-scale GEDI-derived estimates of forest fuel structure (where forest is defined as vegetation ≥ 5 m) to assess fuel structure's effects on wildfire severity patterns, and how these relationships change across a gradient of topographic, fire weather and climate conditions among 42 large (>2000 ha) wildfire burn scars in California from 2019–2021 (Fig. 1; Table S1). Among the many ways to extract information on fuel structure from individual GEDI waveforms, we focused on four particularly promising metrics, each selected for their relative parsimony, interpretability, and representativeness across the primary dimensions of canopy structure^{37,38}. Selected fuel metrics include (1) biomass (specifically, above-ground biomass density; AGBD); (2) canopy height (the relative height of the 98th percentile of returned energy; RH98); (3) canopy layering (the number of distinct modes in the raw waveform; nmode), and (4) ladder fuels (mean plant area index below 10 m; mPAI_{10m}). While total biomass and canopy height are established metrics that quantify critical components of canopy volumes²⁸, GEDI-derived layering and ladder fuels are, to the best of our knowledge, novel indicators of vertical continuity in fuel structure (Fig. 2). These vertical continuity metrics are proposed in response to the demand to better characterize under-represented aspects of vertical fuel continuity, especially in the subcanopy³⁹. Put simply, layering can be envisioned as the total number of distinct canopy layers, such that more layers generally correspond to greater canopy heights as well as greater continuity of fuels from the ground to the top of the canopy (Fig. 2). Ladder fuels, on the other hand, are defined as fuels between 0–10 m that can propagate flames from the ground stratum (0–5 m) to tree crowns (>10 m). Because of the specific requirement for at least three 5 m PAI bins (a result of physical constraints from GEDI's pulse width⁴⁰) from which to define GEDI-based ladder fuels, it is only applicable to forests with canopy heights over 10 m (See Methods: GEDI fuel structure).

Wildfire effects were characterized in terms of severity, which we define as the proportion of aboveground organic matter directly consumed (combusted) by fire⁴¹. This is in contrast to longer-term, lagged ecosystem responses like delayed tree mortality and vegetation resprouting⁴². Owing to the vast size of recent wildfire extents, quantifying burn severity is not easily undertaken nor consistently reconciled across sites. Field indices like the Composite Burn Index (CBI) excel for accurately characterizing site-level severity⁴³. However, because the CBI relies primarily on ocular estimates that may vary by worker and often lacks pre-fire measurements at a burned site (instead relying on nearby forests as a proxy), it is not optimal for consistently characterizing broad-scale severity patterns across fires, regions and years⁴⁴. For large-area assessments, satellite optical imagery provides a means to measure vegetation change by quantifying spectral differences between a pre-fire image (ostensibly, but not always, dominated by green chlorophyll in vegetated areas) and a post-fire image where dark elements like ash and charcoal tend to dominate the spectral signature with increasing levels of severity⁴⁴. As such, we adopted the difference Normalized Burn Ratio (dNBR) index, with per-fire offsets, due to its robust history in the literature and high classification accuracies in relation to field measurements⁴³.

In addition to >830,000 samples of GEDI-derived pre-fire fuel structure and co-located dNBR-based burn severity estimates distributed throughout the study domain, we included coincident data on topography, fire weather and climate in a spatial, hierarchical modeling framework to test the following hypotheses: (H1) GEDI-derived fuel structure metrics are positively related to wildfire severity across a range of wildfires in the California study domain; (H2) the magnitude of the role of fuel structure in driving landscape severity patterns will decline with increasing topographic slope and more intense fire weather conditions; and (H3) the strength of fuel structure's relationship with wildfire severity will decline along topographic and climatic conditions perceived to be more conducive to ignition and fire spread.

Fig. 1 | Study domain. a Spatially continuous 1 km resolution map of GEDI-derived canopy heights (RH98) across three Californian study regions and 42 wildfires from 2019–2021. b August Complex fire with MTBS severity classes. c GEDI footprint sampling prior to Caldor fire, where each 25 m GEDI footprint is colored by its spatial blocking group which controls for spatial autocorrelation among proximate samples.

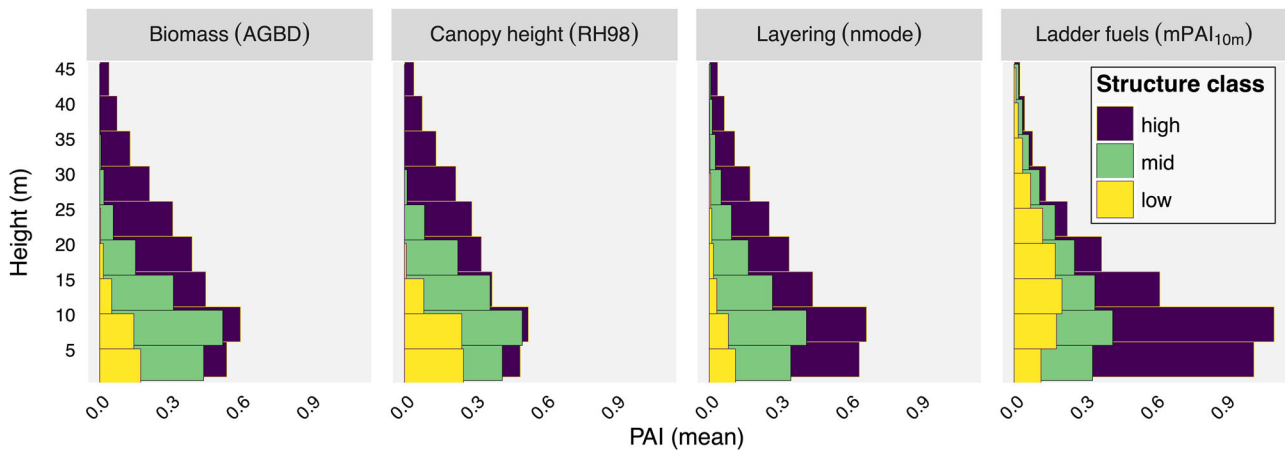
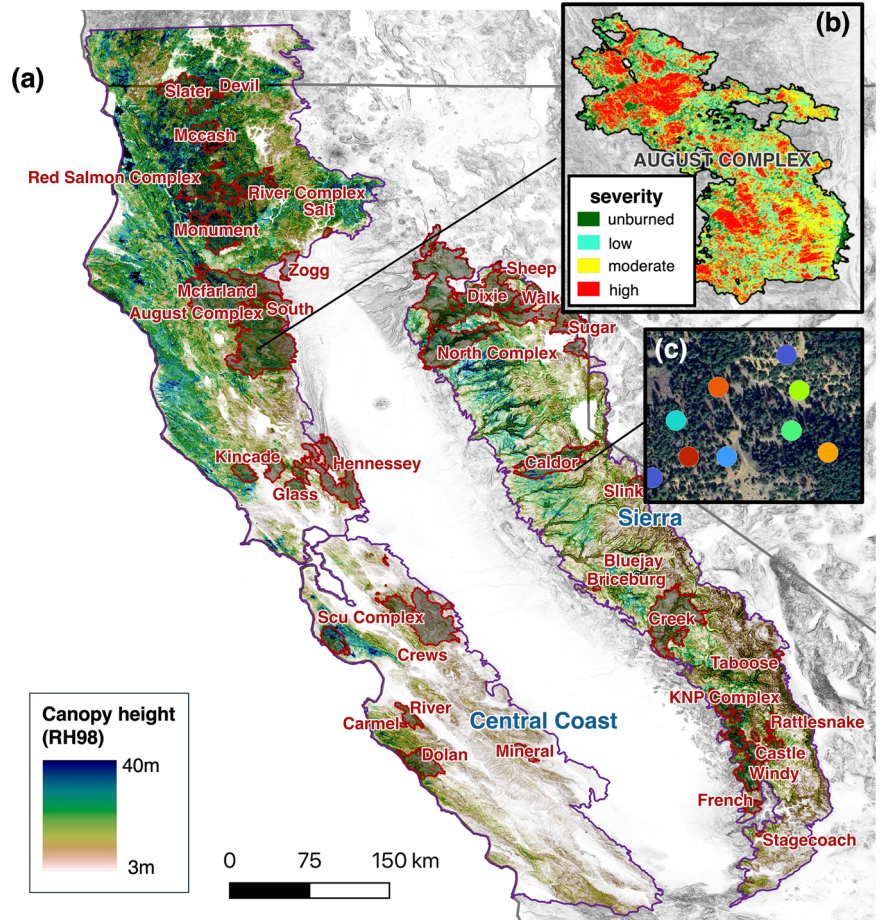


Fig. 2 | Vertical profiles for four GEDI-derived fuel structure metrics, each split into three structural classes. Horizontal bars represent the mean plant area index (PAI) in 5 m vertical height bins from 0–45 m for all GEDI footprints in the study domain. The three structure classes represent percentiles – <33% (low), 33–67%

(mid), and >67% (high) – for each structural metric, and depict how characteristic vertical PAI distributions differ among forests possessing low to high structural attributes for each metric, respectively. See Table 1 for description of metrics.

Results

Fuel structure and wildfire severity

Among the four GEDI-derived forest structural metrics selected for this study, larger values of biomass, canopy height and layering reflect more voluminous canopies as indicated by higher plant area index (PAI) values throughout the vertical profile and into the taller height bins (Fig. 2). Ladder fuels, on the other hand, have pronounced PAI values in the lower forest strata that are not necessarily associated with taller canopy heights.

Generalized Additive Models (GAMs), which employ semi-parametric smoothing functions to characterize the general shape of the relationship between fuel structure and wildfire severity, exhibit functional forms that are consistent with positive, concave-down relationships across all four GEDI-derived fuel metrics (Fig. 3a). Spatial Generalized Linear Mixed Models (spGLMMs), on the other hand, are parameterized with explicit linear and quadratic terms. The spGLMM models corroborate the GAM’s general form, with all four metrics possessing significant linear (positive) and quadratic

(negative) terms (Fig. 3b; S2). Further, all four fuel structural attributes (which depict, to varying extents, the amount and spatial arrangement of forest fuels) positively covary with severity (supporting H1) until they peak at larger relative values of fuel structure (z-score >1), after which the relationship attenuates in the tallest and most voluminous forest canopies.

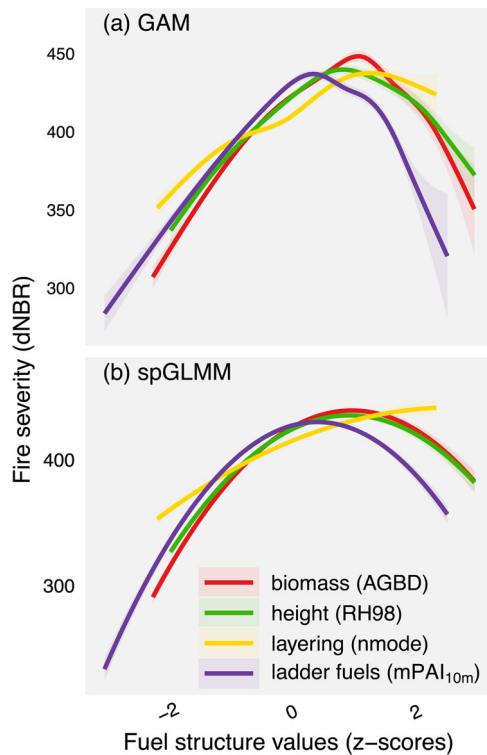


Fig. 3 | Generalized relationships between fuel structure and wildfire severity. a Generalized Additive Models (GAMs) and b spatial GLMM (spGLMMs) quadratic regressions between standardized fuel structure values (z-scores) and wildfire severity based on dNBR. Linear and quadratic coefficients in the four spGLMMs were positive and negative, respectively, and significant at $p < 0.05$ (S2.1).

Fuel structure and topo-weather interactions

A series of multivariate spGLMMs were used to assess the independent (i.e. partial) and interactive effects of fuel structure, topography and fire weather variables on severity patterns across the 42 wildfire burn scars. Consistent with their uniformly positive effect on fire severity in the univariate case (Fig. 3b), fuel structure’s partial spGLMM coefficients were significantly positive in all cases except for canopy height (RH98) after controlling for slope or wind conditions (Fig. 4a).

Topo-weather variables like slope, VPD, ET and wind speed were likewise consistently positively related to fire severity, with the sole exception of ET after accounting for ladder fuels (Fig. 4b). Critically, significant negative interactions were observed for nearly all combinations of fuel structure and topo-weather variables (Fig. 4c). This result is consistent with H2, whereby structure’s positive effects on wildfire severity decrease in more extreme conditions such as steeper slopes, drier weather, and greater wind speeds. Conversely, the greater the fuel structural attributes (e.g. taller, higher biomass forests), the lesser the independent role of topo-weather in determining severity patterns.

Model results obtained from splitting the full dataset into five equal-sized subsets stratified by topographic slope and weather variables indicate that while structure-severity relationships from all data (“all”) were significantly positive, many of these relationships were not significant in extreme topo-weather conditions (Fig. 5). For example, on slopes greater than 20°, where VPD levels were greater than 2.9 kPa, where ET was greater than 1 mm/8days, or where wind speeds were greater than 9.3 m/s, biomass and canopy height were no longer significantly related to severity. Canopy layering, on the other hand, was a consistent predictor of severity across topo-weather conditions, but it too was not significant at ET levels greater than 1 mm/8days, or where wind speeds were moderately high (9.3–11.6 m/s). Importantly, only ladder fuels exhibited consistently significant positive effects on wildfire severity across all topographic slopes and fire weather conditions.

Fuel-severity across topo-climate gradients

While spGLMMs with fire level random effects explicitly account for the hierarchical structure of the dataset across a wide range of wildfires (S1; S3), there was considerable variability in the sign and magnitude of the relationship between fuel structure and fire severity among individual wildfires. To examine factors constraining intra-fire structure-severity relationships,

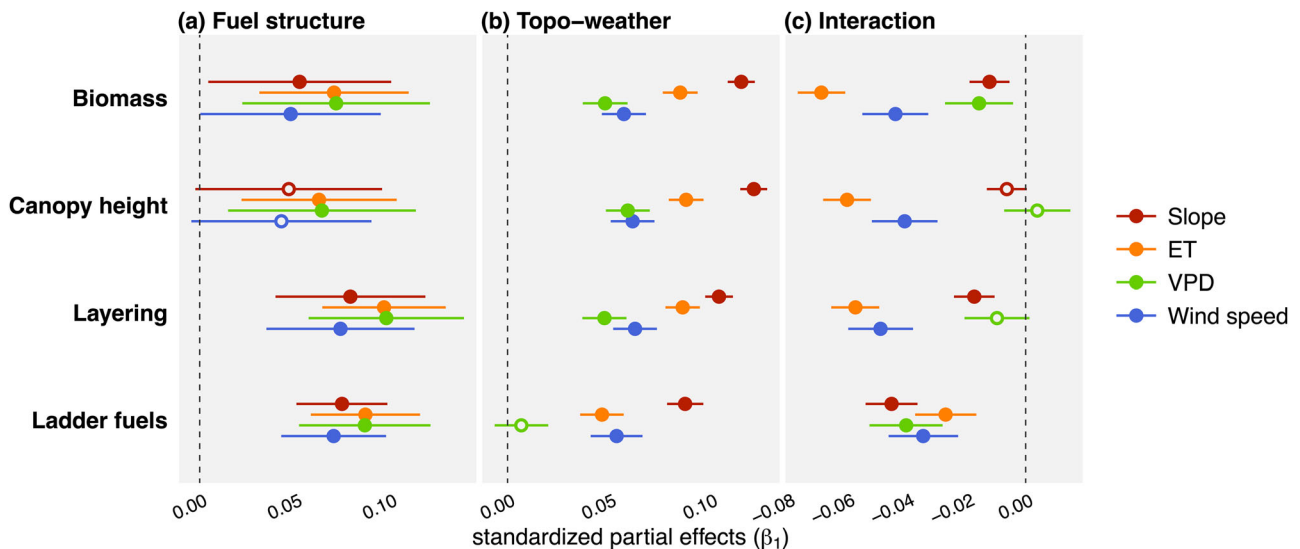


Fig. 4 | Partial and interactive effects of fuel structure and topo-weather on fire severity. Slope estimates (β_1), standardized by z-score, represent the partial linear effects of a) fuel structure, b) topographic and weather variables, or “topo-weather”, and c) their interaction on wildfire severity from a series of spGLMMs. Across all combinations of fuel structure and topo-weather, standardized partial

effects correspond to the linear effect of a given predictor on dNBR-based severity (response) after accounting for the effect of the other predictor, plus its interaction. Median posterior estimate (points) and associated 95% credible interval (error bars); terms not significant (open symbol) when the credible interval includes zero (dashed vertical line).

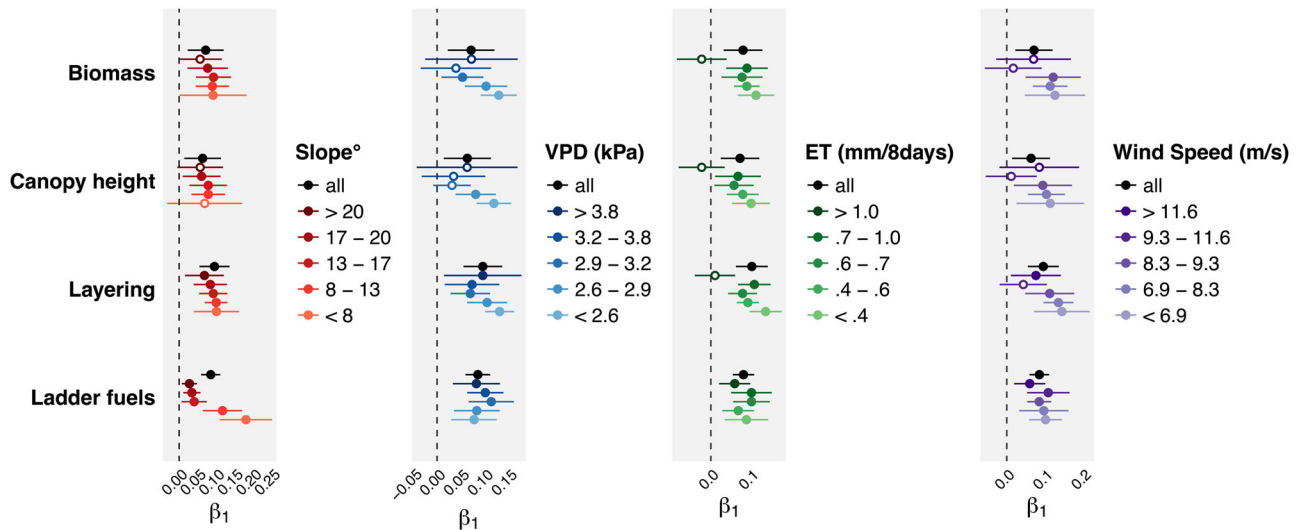


Fig. 5 | Effects of fuel structure on fire severity across five levels of topo-weather. Slope estimates (β_1), standardized by z-score, represent the univariate linear effects of GEDI-derived fuel structural variables on dNBR wildfire severity from a series of spGLMMs. Model results were obtained from all data samples (“all”) in addition to

subsets defined as five equal-sized classes stratified by corresponding topo-weather variables. Median posterior estimate (points) and associated 95% credible interval (error bars); terms not significant (open symbol) when the credible interval includes zero (dashed vertical line).

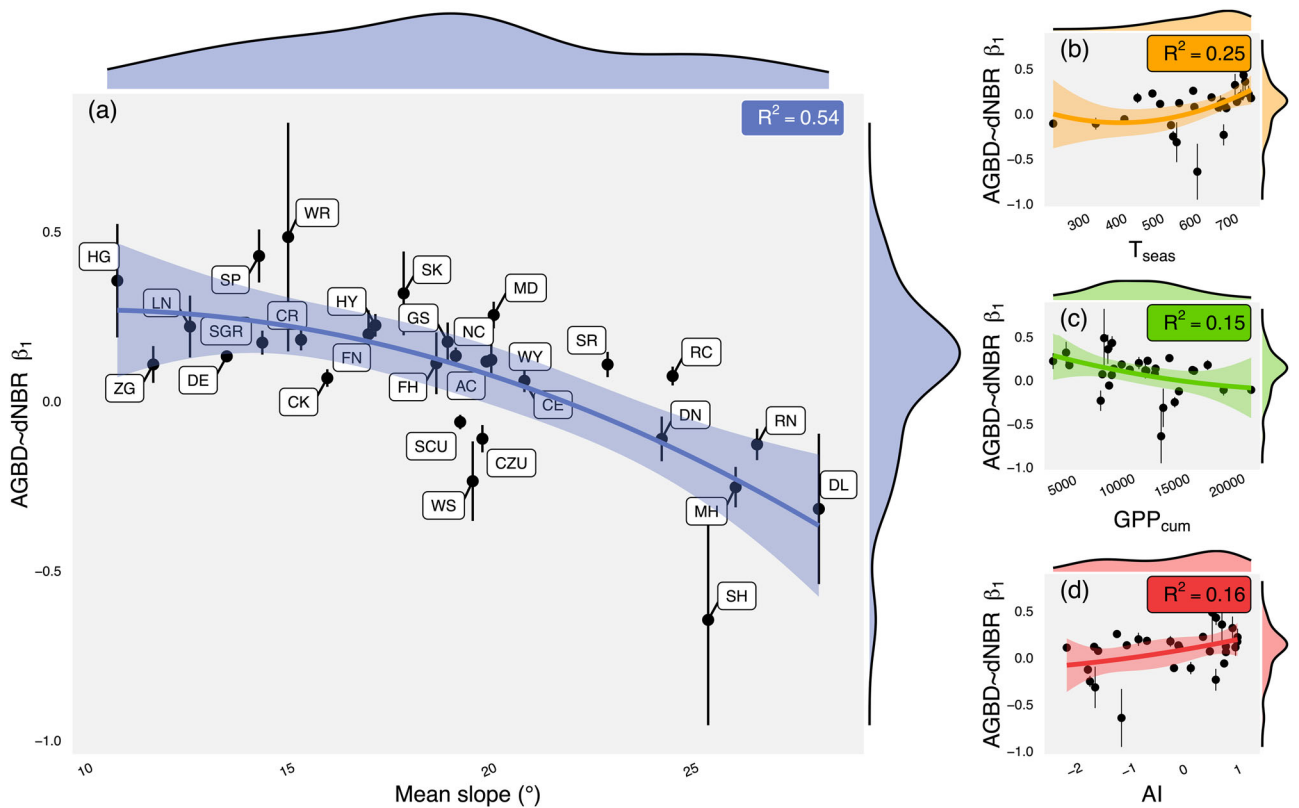


Fig. 6 | Intra-fire effects of forest biomass on fire severity across topographic slope and climate gradients. Subsets depict how intra-fire (i.e. per fire) fuel-severity relationships change across topo-climatic contexts. Specifically, for each wildfire possessing a significant intra-fire linear effect between biomass and severity, its per-fire regression slope coefficient (AGBD~dNBR β_1) was regressed against mean

values of (a) slope; (b) temperature seasonality (T_{seas}); (c) cumulative Gross Primary Productivity (GPP_{cum}); and (d) aridity index (AI) - each corresponding to the entire spatial extent of each fire. See Table 1 for variable descriptions and Table S1 for labeled fire abbreviations for panel (a).

we assessed how per-fire regression slope coefficients change along gradients in topography and climate, using a generalized characterization of fuel volume: biomass (AGBD). We found that standardized intra-fire biomass effects on severity (AGBD~dNBR β_1) tended to decline (e.g., their slope was more negative) along a gradient of higher mean topographic slope.

We also found a decreasing trend with productivity (GPP_{cum}) and concurrently an increasing relationship with temperature seasonality (T_{seas}) and mean aridity (AI) (Fig. 6). While a decreasing role of structure in steeper regions was consistent with expectations from H3, the positive covariance between AGBD~dNBR β_1 coefficients and T_{Seas} and AI values led us to reject

H3. All quadratic relationships exhibited a significant slope and possessed R^2 s of 0.54, 0.15, 0.25, and 0.16, respectively.

Discussion

Based on a dataset of GEDI-derived, pre-fire fuel structure metrics across 42 large wildfires over three years, model results indicate a consistent positive relationship between fuel structure variables (biomass, height, layering, and ladder fuels) and wildfire severity. These findings support H1, which postulated forest fuel's positive relationship with wildfire severity, and tends to corroborate findings from specific case studies^{15,19} as well as some multi-fire assessments^{8,17}. Furthermore, these fuel-severity relationships concurrently possess significant negative quadratic terms, which corresponds to a concave-down relationship. In other words, larger fuel structure values were associated with higher severity burns up until the highest values of fuel structure, after which they were associated with more moderate severity levels.

This reduction in severity for the largest biomass forests is consistent with patterns observed in fire refugia, whereby certain high-biomass areas tend to be repeatedly spared from high severity fire within a matrix of mixed-severity burns³³. Studies have noted the propensity of valley bottoms and local concavities in arid forests to support voluminous, late-seral forests owing to multiple environmental factors including reduced ET due to hillshading, cold air pooling, or higher soil and canopy moisture levels for forest stands in close proximity to streams⁴⁵. At the same time, tall multi-layered canopies transmit less light through the canopy, thereby reducing evaporative demand on the forest floor and creating a moderated microclimate less conducive to ground fire propagation⁴⁶. This observation, whereby larger trees tend to burn less severely, may likewise have bearing on fuels treatment designed to retain and recruit large diameter trees for simultaneous biodiversity and fuel reduction targets⁴⁷.

While the positive relationship between top-of-canopy height and wildfire severity has been corroborated by several other studies^{32,47–49}, this single height metric has limited information content, especially for characterizing the vertical distribution of canopy fuel in structurally-complex forest canopies. Aboveground biomass, on the other hand, provides a more information-rich indicator of total fuel volume. For a given level of fuel moisture, heat output and transfer is greatest for fuels with high surface area relative to volume⁵⁰. Therefore, biomass density (AGBD) has been commonly used as a direct antecedent to common fuel structure parameters such as CBD and CFL, which each reflect biomass above the canopy base height (CBH), or the height at which canopy fuels allow for vertical fire propagation²⁹. However, CBH is an ambiguous concept, in part because it is problematic to accurately and consistently estimate across ecosystems and forest types, and difficult to verify with field measurements³⁹. AGBD, on the other hand, is a consistently estimated GEDI-derived product, validated across plant functional types in the study domain and globally^{51,52}.

Critically, total biomass is agnostic to how forest fuels influence the vertical propagation of fire from the ground to tree crowns. Vertical fuel continuity directly affects flame length and propagation⁵³, but has remained a challenging canopy attribute to consistently estimate, especially across uneven-aged, heterogeneous forests³⁹. To address this gap, we tested nmode as a proxy for structural diversity (but more accurately described as vertical layering). Nmode exploits GEDI's continuous vertical waveform to characterize evenness across vertical strata. Simply described, a greater number of modes in GEDI's waveform corresponds to a larger number of distinct biomass elements across a forest's vertical profile, and hence greater vertical fuel continuity. Unlike more common indices of structural diversity like foliar height diversity (FHD), which is partly derived from the number of pre-established canopy height bins, nmode is not a priori dependent upon canopy height and therefore offers an alternative representation of structural diversity with a degree of independence from RH98, even if the two metrics are correlated (see Fig. S4.3)⁵⁴.

Vertical fuel continuity is especially important for lower stratum ladder fuels, where greater continuity may enable flames to transition from ground and surface fires to higher canopy strata, thereby increasing contagion and

eventual burn severity⁴⁶. As with vertical fuel continuity, studies have noted the difficulty in consistently estimating sub-canopy ladder fuels in the field and across airborne lidar campaigns^{32,39}. These results confirm the ability of GEDI waveforms to consistently estimate lower canopy fuel structure despite challenges with lidar signal attenuation in the lowest reaches of dense, high biomass forests⁵⁵. Furthermore, our finding that a GEDI-derived proxy for ladder fuels, mPAI_{10m}, was the strongest (highest magnitude) and most consistent predictor of severity across topographic and fire weather conditions reinforces the role of ladder fuels as an essential fuel structure metric. Conversely, those forests with less ladder fuels (possessing the lowest mPAI_{10m} values) were the least likely to burn at high severity. While the sample size for ladder fuels was smaller than that of the other three metrics (734,347 GEDI footprints for ladder fuels versus 830,709 for biomass, height and layering; or an 11.6% reduction), this sample size differential had no substantial effect on findings (See S5).

Of particular interest for this study was determining how generalized structure-severity relationships change across topo-weather conditions. A number of studies have found evidence for forest structure overwhelming the effect of topography³⁶, fire weather³², or both^{8,19}. Other studies have found these relationships to vary by context such that fuels dominate during mild weather conditions, while extreme conditions (such as acute drought or high winds) may overwhelm fuel structure in determining severity patterns²⁰. Our results – including significant negative interaction coefficients between structure and topo-weather (Fig. 4) as well as nonsignificant fuel structure coefficients in the most intense topo-weather subsets (Fig. 5) – are consistent with the conclusion of topography- and weather-mediated context dependency. Consistent with expectations from H2, we observed that steep slopes, dry conditions and high winds overwhelmed most fuel structural conditions to constrain landscape severity patterns. Importantly, the sole exception to this pattern occurred with ladder fuels and to a lesser extent, canopy layering.

Quantile values (Fig. 5) provide an indicator of which specific values of topo-weather conditions may serve as a 'switch' between fuel- and topo-weather dominated severity. For example, one study found this transition towards weather-controlled severity to occur at 20–40% relative humidity, though we surmise specific threshold values will fluctuate in different contexts⁴⁸. Importantly, fuel structure may itself feedback upon local climate conditions, such as when dense forest canopies moderate subcanopy microclimatic which serves to slow fire progression regardless of fuel volumes⁴⁶. At the same time, intermediate topo-weather conditions may interact to create more extreme conditions than either on its own, such as when wind direction is perpendicular to topographic aspect for uphill heading fires⁴⁶ or when continental easterlies coincide with VPD minima to drive the rapid spread of high-severity wildfires⁵⁶.

Studies have found a variety of divergent drivers of severity across different ecosystems and along gradients in topography and climate^{34,57}. Our observation that structure-severity effects decline with greater mean topographic slope is consistent with H3 as well as results from GEDI footprint sample analyses (i.e. Fig. 4c). This result suggests fuel structure's diminishing role in constraining fire severity patterns in steeper terrains. Conversely, the increase of intra-fire fuel structure effects along a gradient of increasing aridity and temperature seasonality (a result likewise recently found in western Tasmania)⁵⁸ as well as its decrease with greater productivity, led us to ultimately reject H3. This diverging pattern suggests a change in the relative role of fuel structure in driving fire severity along a spectrum from climate-limited (high biomass but high relative moisture) to fuel-limited (conditions supporting combustion, but limiting biomass growth) ecosystems^{57,59}. Thus, in this analysis, severity was less dependent on fuel structure in high productivity regions where fuels were not limited and where other climatic factors had a larger relative impact on severity patterns. This observation is consistent with a recent study that found that given extreme fire weather conditions, excess fuel volumes and ignition, more productive regions tend to burn at the highest severity levels⁶⁰. Moreover, in fuel-limited arid regions, the relative importance of fuel structure in driving severity may increase where severity patterns more closely track the spatial

footprint of combustible biomass as opposed to non- or sparsely-vegetated surfaces, which tend to arrest fire progression⁶¹.

A few important caveats and considerations should be considered in interpreting these results. First, while dNBR excels as a satellite optical-based index of fire severity⁴³, studies have noted several issues with its use. In forests with sparse cover, variability in subcanopy and ground conditions may confound attempts to differentiate between unburned and low-severity wildfires^{33,42}, while also failing to distinguish stand-replacing fires as high severity⁶². In forests with high canopy cover, optical indices may underestimate understory severity as satellite remote sensing of top-of-canopy reflectance is mostly influenced by photon interaction with upper-canopy features⁴⁹. Furthermore, optical indices are subject to noise depending on date of acquisition (e.g. low sun angles and leaf senescence) and time between fire containment and post-fire observation, such that post-fire grass regrowth or epicormic sprouting limit the detection of the extent of canopy severity given enough time having transpired⁴⁴. Related to this, studies have noted the spectral similarity between fire-induced charcoal and shadow effects in otherwise healthy, structurally-complex vegetation⁶³. Second, this study looked at fuel structure as distinct from fuel condition and horizontal connectivity as they influence landscape fire severity patterns. While this study's sampling and statistical design intrinsically incorporated these latent factors, future research would benefit from a more explicit partitioning of these fuel-related drivers of severity, including 3D spatial contagion of live and dead fuel moisture, and leaf traits like foliar chemical composition. Finally, the time period covered (2019–2021) caps a mega-drought in the region, and the driest 22-year period since 800 CE, with over double the acreage burned than the previous historical record⁶⁴. Thus, while the climate context was relatively consistent across the study duration, this three-year period of GEDI observation may obscure inference into longer-term decadal dynamics, especially under wetter conditions. While it is ill-advised to directly extrapolate results from this study to regions outside of the study domain, future research could address the utility of using climate proxies to assess how relationships between fuels, topo-weather and severity generalize to other regions. For example, does this study's finding that biomass and severity were more tightly coupled in increasingly arid regions hold in other Mediterranean regions? How do differential drivers of fire progression – including wind speed and direction as well as landscape treatment design – affect relationships outside of the study domain? Despite the promise of broad-scale application, GEDI samples – especially in lower latitude regions – may be too sparsely distributed to effectively assess small-medium sized fires (<2000 ha) or where spatio-temporal resolution is critical to management intervention such as when assessing small-scale prescribed burns.

Conclusions

Wildfires, especially mixed-severity burns, can be healthy for maintaining multi-scale landscape ecosystem processes and biodiversity^{1,9,10,65} while suppression efforts may actually accentuate future burn severity⁶⁶. However, climate warming trends have interacted with historically-anomalous forest fuel density and continuity to generate wildfires of increasing size and severity^{6,21,67}. As such, forest management guidelines in the Western US have increasingly prioritized reducing the incidence of high-severity wildfires to minimize the loss of human life and property, and to slow the processes of vegetation type conversion which are exacerbated by climate warming^{12,13,21}. Results from this study confirm the utility of GEDI-derived fuel estimates, including those of ladder fuels, for consistently predicting wildfire severity across large areas, multiple years, and varying topo-weather conditions. Inasmuch as high-quality data on weather conditions is available, GEDI fuel structure metrics provide a novel and complementary tool to guide forest management, including pre-fire treatment and suppression, especially for regions lacking ALS monitoring capabilities^{68,69}.

Furthermore, these findings emphasize the effect of topo-weather thresholds or 'switches', after which fuel structure and fuel treatments may have a diminished role in determining severity patterns⁷⁰. Critically, this

switch from fuel to weather-dominated wildfires was most pronounced for structural metrics associated with canopy volumes (e.g. height and above-ground biomass), while vertical fuel continuity metrics (especially ladder fuels) consistently predicted wildfire severity even in extreme topographic and weather conditions. This finding suggests that high-intensity fuel treatments (which target entire forest canopies rather than focusing on lower stratum ladder fuels only) may have a limited effect on wildfire severity in extreme conditions. Conversely, sparse understories (<10 m) – even those that concurrently possess robust mid- strata (>10 m) – were associated with reduced wildfire severity. This result has important management implications, especially for treatment interventions that focus on vertical fuel continuity such as understory thinning or cultural burns, which have been found to be effective in reducing high-severity burns². Understory treatments have also been found to lessen externalities associated with more intensive thinning operations⁷¹ and simultaneously promote culturally- and ecologically-beneficial wildfire outcomes across a wide variety of topographic, weather and climate contexts^{1,72}.

Methods

Study domain

The study domain was defined as the North Coast, Central Coast, and Sierras regions of California (Fig. 1), for fires occurring during years of temporally-coincident GEDI observations; namely, 2019–2021. California is the most fire-prone state in the lower USA, and supports the most fire-adapted vegetation⁶⁴. The study domain is an environmentally-varied mountainous region, with elevations ranging from 10 m below sea level to 4413 m and mean annual temperatures ranging from -3.4 – 19 °C (Fig. 1). Apart from the higher elevation Sierras and coastal temperate rainforests, most of the study domain possesses a Mediterranean climate with ample precipitation in the winter, vigorous growth in spring, and hot and dry summer-autumn periods. Sampled vegetation in this study can be characterized primarily sclerophyllous shrublands, oak woodlands, and conifer forests (>5 m) where composition tends to track climate and elevation gradients.

Data and sampling

This study employed pre-fire structure derived from GEDI waveforms as well as spatially coincident data on topography, fire weather, climate and dNBR-based burn severity (Table 1). All data consist of 45 m diameter circular samples centered on the estimated centroid location of each GEDI footprint. The 45 m diameter extent of each sample was determined from the 25 m diameter circular GEDI footprint, buffered outwards by 10 m to account for potential geolocal error, estimated as ± 10 m (1 standard deviation)⁷³. All samples were extracted from within the perimeter of all large (>2000 ha) wildfires in the study domain buffered inwards by 90 m to minimize edge effects and geolocation imprecision.

GEDI fuel structure

The GEDI space-borne lidar sensor produces high resolution laser ranging waveform profiles for monitoring near-global vegetation structure²⁷. GEDI L2A, L2B and L4A version 2 data^{40,51,74,75} were filtered to include only high quality shots, defined as: (1) possessing a minimum canopy height (RH100) of 5 m; (2) having been acquired during leaf-on dates (corresponding to day of year 105 to 319); (3) occurring on slopes less than 25° owing to challenges with ground-finding in steep terrain; (4) possessing footprint elevations <150 m divergent from a TanDEM-X digital elevation model to prevent the erroneous inclusion of low-lying clouds; (5) having minimal positional degradation as indicated by the degrade flag; (6) possessing surface flag equal to 1 and the stale return flag equal to 0; and (7) having beam sensitivity >0.9 for the default ground finding algorithm and sensitivity of >0.95 for ground finding algorithm²⁷. Among all GEDI waveform shots selected from within the study domain, those occurring within the extent of two overlapping wildfire scars within the last ten years, or identified as non-forest from CALVEG vegetation maps, were excluded⁷⁷. In total, these criteria constrained our dataset to 830,709 samples across 42 large wildfires (Fig. 1; Table S1).

Table 1 | Data, metrics and definitions

Category	Metric	Definition	Abbr.	Units
Forest fuel structure	Biomass	Total above-ground biomass from GEDI waveforms (L4A) ^{51,74}	AGBD	m/m ²
	Canopy height	Relative height of the 98th percentile of returned energy from GEDI waveforms (L2A) ⁷⁵	RH98	m
	Layering	Number of modes in the GEDI waveform (L2B) ⁴⁰	nmode	<i>n</i>
	Ladder fuels	Mean plant area index (mPAI) for 5 m vertical increments below 10 m for canopies >10 m (L2B) ⁴⁰	mPAI _{10m}	m ² / m ²
Fire weather	Evapo-transpiration	Weighted mean values from 8-day, interpolated from 1 km gap-filled MODIS (MOD16GF) global evapotranspiration	ET	mm / 8 days
	Vapor pressure deficit	Weighted mean daily values in the month preceding ignition interpolated from 4 km gridMET ⁸³	VPD	kPa
	Wind speed	Weighted mean daily values during wildfire interpolated from 4 km gridMET ⁸³	--	m/s
Topography	Slope	Weighted mean slope derived from the USGS National Elevation Dataset ⁸²	--	degrees
Climate	Temperature seasonality	Standard deviation of monthly temperature per annum at 1 km resolution ⁸⁵	T _{seas}	sd °C
	Productivity	Cumulative Gross Primary Productivity from 1 km MODIS (MOD13A2) summed over 2003-2014 ⁸⁷	GPP _{cum}	kg C / m ²
	Aridity	Global aridity index calculated as normalized annual precipitation / ET at 1 km resolution ⁸⁶	AI	unitless

From many potential GEDI-derived canopy metrics⁷⁸, four were selected for analysis (1) aboveground biomass, or biomass, from GEDI's L4A aboveground biomass density (AGBD) product⁵¹; as well as L2A and L2B derived products, including: (2) canopy height, or the 98 percentile of relative heights (RH98); (3) canopy layering based on the number of modes in the raw GEDI waveform profile (nmode); and (4) ladder fuels, which we characterize using the mean PAI below 10 m, for all canopies with RH98 > 10 m (mPAI_{10m}) (Table 1). Biomass and height are common indicators of fuel volumes^{37,38}, while layering and ladder fuels are GEDI-determined indicators of vertical continuity in fuel structure (despite significant correlation; Fig. S4.3). Importantly, ladder fuel metrics are only applicable for forests >10m due to the physical constraints of GEDI's pulse width, which is optimized for detection of PAI in 5 m vertical bins⁴⁰. This 5 m binning size likewise balances the need for a sufficient signal from which to accurately characterize PAI (an aggregate value of plant area in a pre-defined volume) while still providing the best possible vertical resolution. Because of this GEDI-determined constraint, ladder fuels are defined as the amount of canopy fuels between 0–10 m that can serve to propagate flames from one 5 m layer below (the 0–5 m ground stratum) to one layer above (tree crowns >10 m)⁷⁹. Therefore, the sample size for ladder fuels was smaller than that of the other three metrics (734,347 GEDI footprints for ladder fuels versus 830,709 for biomass, height and layering; or an 11.6% reduction in sample size; See S5).

While most GEDI-derived fuel structure metrics possess varying degrees of correlation (See Fig. S4.3), the aforementioned four metrics were chosen based on the following criteria: (a) they should be easily interpretable to remote sensing and fire science research and management communities, (b) they should be well-distributed across a range of canopy height, volume and heterogeneity categories³⁷, (c) they should each show promise to independently predict wildfire severity across the study domain, and (d) they should balance precedence in the literature with novelty for new predictors. Thus, while total biomass and canopy height are well-established in the literature^{28,37}, GEDI-derived layering and ladder fuels are, to the best of our knowledge, novel metrics proposed to better characterize under-represented aspects of vertical fuel continuity, especially in the subcanopy³⁹.

Wildfire severity, topography, fire weather, and climate data

Wildfire severity was characterized from the 30 m resolution Monitoring Trends in Burn Severity (MTBS) dNBR product⁸⁰, with per-fire offsets applied⁸¹. In preliminary testing, we found that dNBR outperformed MTBS's discrete severity classes, the Relativized dNBR (RdNBR), as well as logarithmic Composite Burn Index (CBI) transformations based on dNBR. From the 30 m resolution dNBR raster, we extracted an area-based weighted average for each 45 m circular sample across all corresponding pixels, and in

proportion to the area covered by each pixel's value in the 45 m sample. Topographic slope (°) was derived from the 10 m USGS National Elevation Dataset⁸². Slope values corresponding to 45 m diameter samples adopted averages across all corresponding 10 m pixels, weighted by the proportion of each 10 m pixel in each circular sample.

VPD and wind speed were derived from daily, 4 km gridMET rasters and spatially interpolated to specific GEDI footprint locations. GridMET blends spatial data from PRISM with daily National Land Data Assimilation System data⁸³. VPD (kPa) and wind speed (m/s) were derived as the maximum daily value for each wildfire's duration (between alarm and containment dates). Spatial interpolation was employed on all gridMET variables to derive unique values for each 45 m sample based on area-to-point kriging (ATPK), which relies on a sample's relative location within a given pixel, in addition to its Euclidean distance to neighboring pixels to estimate an interpolated weighted average⁸⁴. ET (mm / 8 days) was derived as the mean value of 8-day, 1 km gap-filled MODIS global ET (MOD16GF) for the month prior to ignition. We employed quality-filtering on all ET data to remove pixels flagged as "significant clouds present" or "mixed clouds".

Climate indices were compiled from 1 km resolution global climate products representing mean conditions between 1979 and 2013 for the entire extent of each wildfire^{85,86}. Temperature seasonality was expressed as the standard deviation in monthly mean temperature (T_{seas})⁸⁵. The aridity index (AI) corresponds to moisture availability for potential growth of reference vegetation excluding the impact of soil mediating water runoff events⁸⁶. AI was calculated as annual precipitation divided by ET, multiplied by -1 so that AI values increase with aridity, normalized by z-score, and centered on 0⁸⁶. For cumulative gross primary productivity (GPP_{cum}), we adopted the corresponding dynamic habitat index (DHI) which consists of the median of all good GPP observations from the MODIS GPP product (MOD17A2) between 2003–2014⁸⁷.

Spatial hierarchical models

Prior to model application, all variables were assessed for violations from the normal distribution based on the Shapiro-Wilks statistic (*W*). When variables significantly deviated from a normal distribution, we employed Tukey's Ladder of Powers and cycled through transformation coefficients (λ), selecting the λ value that maximized *W*, and used it to transform the raw vectors to a normal distribution. For cross-comparison among variables in different units and scales, all variables were standardized based on z-score and centered around zero, with those variables exhibiting a z-score greater than 4 removed as outliers.

GEDI footprint locations exhibit a non-random, linear, lattice-like spatial structure whose spatial dependence could violate assumptions of independence underlying our parametric modeling framework and

potentially underestimate model prediction error. To test for a spatial dependence structure among samples, we conducted a Moran's I test on all GEDI structure metrics, finding evidence of spatial autocorrelation for all four metrics. We therefore implemented a spatial blocking routine to remove autocorrelated GEDI shots while providing a framework for permutation-based inference. Spatial blocking, where data are split into groups based on a minimum threshold pairwise distance, has been found to mitigate spatial dependence structures while minimizing data decimation⁸⁸. To do this, we first developed empirical semivariograms for canopy height (RH98) for each fire. RH98 was used for this assessment of spatial autocorrelation because tests have shown it to be the most accurate among our selected canopy structural attributes based on independent validation with a global data set of field sites and airborne lidar⁷⁶.

We then applied a pairwise distance filter initiated from the semivariogram range so that only points beyond that nominal Euclidean distance were retained for a secondary Moran's I test. When significant (i.e. autocorrelated), we iterated larger blocking distances until remaining points produced a non-significant Moran's I . This process was repeated ten times (with replacement) for each wildfire, each initiated with a different random seed, to produce ten distinct GEDI sample combinations per fire, whereby all shots in each of the ten sample sets were sufficiently uncorrelated as determined from re-evaluated Moran's I values. All subsequent models were iterated over each of the ten sample sets to produce mean ensemble coefficient estimates (including intercepts, slopes, and standard errors) based on the resulting distributions.

Inference into underlying relationships was predicated on univariate and multivariate hierarchical spatial Generalized Linear Mixed Models (spGLMMs). Both univariate (Fig. 3) and multivariate (Figs. 4, 5) spGLMMs were parameterized with random intercepts and random slopes, with random effects determined at the level of the wildfire. Univariate spGLMMs incorporated two terms for each predictor: a linear and a quadratic term. Multivariate spGLMMs, on the other hand, included a structural variable, a topo-weather variable, and an interaction term – each run in a series based on all pairwise combinations of structural and topo-weather variables. Only fires with >500 shots per seed/fire were included as a random effect. For Fig. 5, all data samples were subset into five equal-sized quantiles stratified according to topographic and weather values, and then subjected to multivariate spGLMMs as above. Finally, for each wildfire possessing a significant intra-fire linear effect between biomass and severity, z -score standardized intra-fire regression slope coefficients between biomass and severity were regressed against mean topo-climate conditions across each fire's extent. Unlike prior models, intra-fire quadratic linear regressions employed a single response (AGBD~dNBR β_1) and a single predictor, representing the mean climate condition across the fire extent. All GLMMs were run in the nlme⁸⁹ package in R⁹⁰.

Reporting summary

Further information on research design is available in the Nature Portfolio Reporting Summary linked to this article.

Data availability

All datasets used are publicly available. The GEDI L2 dataset is available from the LP DAAC (https://lpdaac.usgs.gov/products/gedi02_av002/, https://lpdaac.usgs.gov/products/gedi02_bv002/) and the L4 dataset is available from the ORNL DAAC. All open access data for this study were downloaded from the following websites: CHELSA, <https://chelsa-climate.org>; AI, <https://cgicrsi.community/data/global-aridity-and-pet-database/gridMET>, <https://www.climatologylab.org/gridmet.html>; MODIS ET, <https://lpdaac.usgs.gov/products/mod16a2gfv006/>; and Dynamic Habitat Indices, <https://silvis.forest.wisc.edu/data/dhis/>; CALVEG, <https://www.fs.usda.gov/detail/r5/landmanagement/resourcemanagement/?cid=stelprdb5347192>; MTBS, <http://mtbs.gov/direct-download>.

Code availability

All of the code used to develop these analyses is openly available at: <https://zenodo.org/records/14019188>⁷⁸.

Received: 2 July 2024; Accepted: 8 November 2024;

Published online: 20 November 2024

References

- Barros, A. M., Ager, A. A., Day, M. A., Krawchuk, M. A. & Spies, T. A. Wildfires managed for restoration enhance ecological resilience. *Ecosphere* **9**, e02161 (2018).
- Lake, F. K. et al. Returning fire to the land: celebrating traditional knowledge and fire. *J. Forestry* **115**, 343–353 (2017).
- Stephens, S. L., Martin, R. E. & Clinton, N. E. Prehistoric fire area and emissions from California's forests, woodlands, shrublands, and grasslands. *Ecol. Manag.* **251**, 205–216 (2007).
- Iglesias, V., Balch, J. K. & Travis, W. R. U.S. fires became larger, more frequent, and more widespread in the 2000s. *Sci. Adv.* **8**, eabc0020 (2022).
- North, M. P. et al. Operational resilience in western US frequent-fire forests. *Ecol. Manag.* **507**, 120004 (2022).
- Williams, A. P. et al. Observed impacts of anthropogenic climate change on wildfire in California. *Earth's Future* **7**, 892–910 (2019).
- Hagmann, R. K. et al. Evidence for widespread changes in the structure, composition, and fire regimes of western North American forests. *Ecol. Appl.* **31**, e02431 (2021).
- Parks, S. A. et al. High-severity fire: evaluating its key drivers and mapping its probability across western US forests. *Environ. Res. Lett.* **13**, 044037 (2018).
- Perry, D. A. et al. The ecology of mixed severity fire regimes in Washington, Oregon, and Northern California. *Ecol. Manag.* **262**, 703–717 (2011).
- Parks, S. A., Holsinger, L. M., Miller, C. & Nelson, C. R. Wildland fire as a self-regulating mechanism: the role of previous burns and weather in limiting fire progression. *Ecol. Appl.* **25**, 1478–1492 (2015).
- Lesmeister, D. B. et al. Mixed-severity wildfire and habitat of an old-forest obligate. *Ecosphere* **10**, e02696 (2019).
- Guterman, C. H. et al. Vegetation type conversion in the US Southwest: frontline observations and management responses. *Fire Ecol.* **18**, s42408–022–00131–w (2022).
- Harvey, B. J., Donato, D. C. & Turner, M. G. High and dry: post-fire tree seedling establishment in subalpine forests decreases with post-fire drought and large stand-replacing burn patches: drought and post-fire tree seedlings. *Glob. Ecol. Biogeogr.* **25**, 655–669 (2016).
- Keeley, J. E. & Syphard, A. D. Twenty-first century California, USA, wildfires: fuel-dominated vs. wind-dominated fires. *Fire Ecol.* **15** (2019).
- Kane, V. R. et al. Mixed severity fire effects within the Rim fire: relative importance of local climate, fire weather, topography, and forest structure. *Ecol. Manag.* **358**, 62–79 (2015).
- Povak, N. A., Kane, V. R., Collins, B. M., Lydersen, J. M. & Kane, J. T. Multi-scaled drivers of severity patterns vary across land ownerships for the 2013 Rim Fire, California. *Landsc. Ecol.* **35**, 293–318 (2020).
- Walker, X. J. et al. Fuel availability not fire weather controls boreal wildfire severity and carbon emissions. *Nat. Clim. Change* **10**, 1130–1136 (2020).
- Clark, J. S. et al. The impacts of increasing drought on forest dynamics, structure, and biodiversity in the United States. *Glob. Change Biol.* **22**, 2329–2352 (2016).
- Harris, L. & Taylor, A. H. Previous burns and topography limit and reinforce fire severity in a large wildfire. *Ecosphere* **8**, e02019 (2017).
- Lydersen, J. M., North, M. P. & Collins, B. M. Severity of an uncharacteristically large wildfire, the Rim Fire, in forests with relatively restored frequent fire regimes. *Ecol. Manag.* **328**, 326–334 (2014).
- Prichard, S. J. et al. Adapting western North American forests to climate change and wildfires: 10 common questions. *Ecol. Appl.* **31**, e02433 (2021).
- Whelan, A. W., Cannon, J. B., Bigelow, S. W., Rutledge, B. T. & Sánchez Meador, A. J. Improving generalized models of forest

- structure in complex forest types using area- and voxel-based approaches from lidar. *Remote Sens Environ.* **284**, 113362 (2023).
23. Morgan, P. et al. Challenges of assessing fire and burn severity using field measures, remote sensing and modelling. *Int. J. Wildland Fire* **23**, 1045–1060 (2014).
 24. Szpakowski, D. & Jensen, J. A review of the applications of remote sensing in fire ecology. *Remote Sens* **11**, 2638 (2019).
 25. Reeves, M. C., Ryan, K. C., Rollins, M. G. & Thompson, T. G. Spatial fuel data products of the LANDFIRE Project. *Int. J. Wildland Fire* **18**, 250 (2009).
 26. Dubayah, R. et al. GEDI launches a new era of biomass inference from space. *Environ. Res. Lett.* **17**, 095001 (2022).
 27. Dubayah, R. et al. The global ecosystem dynamics investigation: high-resolution laser ranging of the earth's forests and topography. *Sci. Remote Sens* **1**, 1–14 (2020).
 28. Aragonese, E., Garcia, M., Ruiz-Benito, P. & Chuvieco, E. Mapping forest canopy fuel parameters at European scale using spaceborne LiDAR and satellite data. *Remote Sens Environ.* **303**, 114005 (2024).
 29. Garcia, M. et al. Characterization of canopy fuels using ICESat/GLAS data. *Remote Sens Environ.* **123**, 81–89 (2012).
 30. Chen, B. et al. Climate, Fuel, and Land Use Shaped the Spatial Pattern of Wildfire in California's Sierra Nevada. *J. Geophys. Res. Biogeosci.* **126**, e2020JG005786 (2021).
 31. Pascolini-Campbell, M., Lee, C., Stavros, N. & Fisher, J. B. ECOSTRESS reveals pre-fire vegetation controls on burn severity for Southern California wildfires of 2020. *Glob. Ecol. Biogeogr.* 1–14 (2022).
 32. Viedma, O. et al. Disentangling the role of prefire vegetation vs. burning conditions on fire severity in a large forest fire in SE Spain. *Remote Sens Environ.* **247**, 111891 (2020).
 33. Meddens, A. J. H. et al. Fire refugia: what are they, and why do they matter for global change? *BioScience* (2018).
 34. Fernández-Guisuraga, J. M., Suárez-Seoane, S., García-Llamas, P. & Calvo, L. Vegetation structure parameters determine high burn severity likelihood in different ecosystem types: A case study in a burned Mediterranean landscape. *J. Environ. Manag* **288**, 112462 (2021).
 35. McKinney, S. T., Abrahamson, I., Jain, T. & Anderson, N. A systematic review of empirical evidence for landscape-level fuel treatment effectiveness. *Fire Ecol.* **18**, 21 (2022).
 36. Safford, H. D., Schmidt, D. A. & Carlson, C. H. Effects of fuel treatments on fire severity in an area of wildland–urban interface, Angora Fire, Lake Tahoe Basin, California. *Ecol. Manag* **258**, 773–787 (2009).
 37. Atkins, J. et al. Integrating forest structural diversity measurement into ecological research. *Ecosphere* **14**, e4633 (2023).
 38. Hakkenberg, C. R. et al. Inferring alpha, beta, and gamma plant diversity across biomes with GEDI spaceborne lidar. *Environ. Res. Ecol.* **2**, 035005 (2023).
 39. Kramer, H. et al. Estimating ladder fuels: a new approach combining field photography with LiDAR. *Remote Sens* **8**, 766 (2016).
 40. Dubayah, R. et al. GEDI L2B Canopy Cover and Vertical Profile Metrics Data Global Footprint Level V002, distributed by NASA EOSDIS Land Processes DAAC. (2021).
 41. Keeley, J. E. Fire intensity, fire severity and burn severity: a brief review and suggested usage. *Int. J. Wildland Fire* **18**, 116–126 (2009).
 42. Cansler, C. A. & McKenzie, D. Climate, fire size, and biophysical setting control fire severity and spatial pattern in the northern Cascade Range, USA. *Ecol. Appl.* **24**, 1037–1056 (2014).
 43. Miller, C. W., Harvey, B. J., Kane, V. R., Moskal, L. M. & Alvarado, E. Different approaches make comparing studies of burn severity challenging: a review of methods used to link remotely sensed data with the Composite Burn Index. *Int. J. Wildland Fire* **32**, 449–475 (2023).
 44. Key, C. H. Ecological and sampling constraints on defining landscape fire severity. *Fire Ecol.* **2**, 34–59 (2006).
 45. Krawchuk, M. A. et al. Topographic and fire weather controls of fire refugia in forested ecosystems of northwestern North America. *Ecosphere* **7**, e01632 (2016).
 46. Falk, D. A., Miller, C., McKenzie, D. & Black, A. E. Cross-scale analysis of fire regimes. *Ecosystems* **10**, 809–823 (2007).
 47. Alexander, J. D., Seavy, N. E., Ralph, C. J. & Hogoboom, B. Vegetation and topographical correlates of fire severity from two fires in the Klamath-Siskiyou region of Oregon and California. *Int. J. Wildland Fire* **15**, 237 (2006).
 48. Gale, M. G., Cary, G. J., Van Dijk, A. I. J. M. & Yebra, M. Untangling fuel, weather and management effects on fire severity: Insights from large-sample LiDAR remote sensing analysis of conditions preceding the 2019–20 Australian wildfires. *J. Environ. Manag.* **348**, 119474 (2023).
 49. Gale, M. G. & Cary, G. J. What determines variation in remotely sensed fire severity? Consideration of remote sensing limitations and confounding factors. *Int. J. Wildland Fire* **31**, 291–305 (2022).
 50. Albin, F. A. A model for fire spread in wildland fuels by-radiation. *Combust. Sci. Technol.* **42**, 229–258 (1985).
 51. Duncanson, L. et al. Aboveground biomass density models for NASA's Global Ecosystem Dynamics Investigation (GEDI) lidar mission. *Remote Sens Environ.* **270**, 112845 (2022).
 52. Bruening, J., May, P., Armston, J. & Dubayah, R. Precise and unbiased biomass estimation from GEDI data and the US Forest Inventory. *Front. For. Glob. Change* **6**, 1149153 (2023).
 53. Zylstra, P. et al. Biophysical mechanistic modelling quantifies the effects of plant traits on fire severity: species, not surface fuel loads, determine flame dimensions in eucalypt forests. *PLOS ONE* **11**, e0160715 (2016).
 54. Conto, T., de, Dubayah, R. & Armston, J. Characterizing the structural complexity of the Earth's forests with spaceborne lidar. *Nat. Commun.* **15**, 8116 (2024).
 55. Mutanga, O., Masenyama, A. & Sibanda, M. Spectral saturation in the remote sensing of high-density vegetation traits: a systematic review of progress, challenges, and prospects. *ISPRS J. Photogramm. Remote Sens* **198**, 297–309 (2023).
 56. Reilly, M. J. et al. Cascadia burning: the historic, but not historically unprecedented, 2020 wildfires in the Pacific Northwest. *USA Ecosphere* **13**, e4070 (2022).
 57. Steel, Z. L., Safford, H. D. & Viers, J. H. The fire frequency-severity relationship and the legacy of fire suppression in California forests. *Ecosphere* **6**, 1–23 (2015).
 58. Rodriguez-Cubillo, D., Jordan, G. J. & Williamson, G. J. Using multi-decadal satellite records to identify environmental drivers of fire severity across vegetation types. *Remote Sens Earth Syst. Sci.* **5**, 165–184 (2022).
 59. Keeley, J. E. & Syphard, A. D. Different historical fire–climate patterns in California. *Int. J. Wildland Fire* **26**, 253 (2017).
 60. Coppoletta, M. et al. Fire history in northern Sierra Nevada mixed conifer forests across a distinct gradient in productivity. *Fire Ecol.* **20**, 86 (2024).
 61. Krawchuk, M. A. & Moritz, M. A. Constraints on global fire activity vary across a resource gradient. *Ecology* **92**, 121–132 (2011).
 62. Miller, J. D. & Thode, A. E. Quantifying burn severity in a heterogeneous landscape with a relative version of the delta Normalized Burn Ratio (dNBR). *Remote Sens Environ.* **109**, 66–80 (2007).
 63. Pfoch, K. A., Pflugmacher, D., Okujeni, A. & Hostert, P. Mapping forest fire severity using bi-temporal unmixing of Sentinel-2 data - Towards a quantitative understanding of fire impacts. *Sci. Remote Sens* **8**, 100097 (2023).
 64. Safford, H. D. et al. The 2020 California fire season: a year like no other, a return to the past or a harbinger of the future? *Glob. Ecol. Biogeogr.* **31**, 2005–2025 (2022).
 65. Keane, R. E. & Karau, E. Evaluating the ecological benefits of wildfire by integrating fire and ecosystem simulation models. *Ecol. Model* **221**, 1162–1172 (2010).
 66. Kreider, M. R. et al. Fire suppression makes wildfires more severe and accentuates impacts of climate change and fuel accumulation. *Nat. Commun.* **15**, 2412 (2024).

67. van Mantgem, P. J. et al. Climatic stress increases forest fire severity across the western United States. *Ecol. Lett.* **16**, 1151–1156 (2013).
68. Dorado-Roda, I. et al. Assessing the accuracy of GEDI data for canopy height and aboveground biomass estimates in mediterranean forests. *Remote Sens* **13**, 2279 (2021).
69. Li, X. et al. Validating GEDI tree canopy cover product across forest types using co-registered aerial LIDAR data. *ISPRS J. Photogramm. Remote Sens* **207**, 326–337 (2024).
70. Balch, J. et al. Switching on the Big Burn of 2017. *Fire* **1**, 17 (2018).
71. Cochrane, M. A. et al. Fuel treatment effectiveness in the United States. *JFSP Res. Proj. Rep.* **89**, 46 (2013).
72. Zylstra, P. J., Bradshaw, S. D. & Lindenmayer, D. B. Self-thinning forest understoreys reduce wildfire risk, even in a warming climate. *Environ. Res. Lett.* **17**, 044022 (2022).
73. Tang, H. et al. Evaluating and mitigating the impact of systematic geolocation error on canopy height measurement performance of GEDI. *Remote Sens Environ.* **291**, 113571 (2023).
74. Dubayah, R. et al. GEDI L4A footprint level aboveground biomass density, Version 2.1. ORNL DAAC, Oak Ridge, Tennessee, USA. (2022).
75. Dubayah, R. et al. GEDI L2A Elevation and Height Metrics Data Global Footprint Level V002, distributed by NASA EOSDIS Land Processes DAAC, (2021).
76. Burns, P., Hakkenberg, C. R. & Goetz, S. J. Multi-resolution gridded maps of vegetation structure from GEDI. *Sci. Data* **11**, 881 (2024).
77. Sawyer, J., Keeler-Wolf, T. & Evans, J. M. A manual of California Vegetation, Second Edition. Sacramento: California Native Plant Society Press. (2009).
78. Hakkenberg, C. R. Code and data accompanying Hakkenberg et al. (2024). Ladder fuels rather than canopy volumes consistently predict wildfire severity even in extreme topographic-weather conditions. <https://doi.org/10.5281/zenodo.13743422> (2024).
79. Forbes, B. et al. Comparing remote sensing and field-based approaches to estimate ladder fuels and predict wildfire burn severity. *Front Glob. Change* **5**, 818713 (2022).
80. MTBS Project. *MTBS data access: fire level geospatial data*. <http://mtbs.gov/direct-download> (2022).
81. Parks, S., Dillon, G. & Miller, C. A new metric for quantifying burn severity: the relativized burn ratio. *Remote Sens.* **6**, 1827–1844 (2014).
82. Gesch, D. B., Evans, G. A., Oimoen, M. J. & Arundel, S. The national elevation dataset. in *American Society for Photogrammetry and Remote Sensing*, **68**, 5–32 (2018).
83. Abatzoglou, J. T., Williams, A. P. & Barbero, R. Global emergence of anthropogenic climate change in fire weather indices. *Geophys Res Lett.* **46**, 326–336 (2019).
84. Kyriakidis, P. C. A geostatistical framework for area-to-point spatial interpolation. *Geogr. Anal.* **36**, 259–289 (2004).
85. Karger, D. N. et al. Climatologies at high resolution for the earth's land surface areas. *Sci. Data* **4**, 1–20 (2017).
86. Trabucco, A. & Zomer, R. J. Global aridity index and potential evapotranspiration (ET0) climate database v2. *CGIAR Consortium for Spatial Information (CGIAR-CSI)*. 1–10 (2018).
87. Radeloff, V. C. et al. The dynamic habitat indices (DHIs) from MODIS and global biodiversity. *Remote Sens Environ.* **222**, 204–214 (2019).
88. Roberts, D. R. et al. Cross-validation strategies for data with temporal, spatial, hierarchical, or phylogenetic structure. *Ecography* **40**, 913–929 (2017).
89. Pinheiro, J. & Bates, D. nlme: Linear and nonlinear mixed effects models. R package version 3.1–157, <https://CRAN.R-project.org/package=nlme> (2022).
90. R. Core Development Team. R: A language and environment for statistical computing. R Foundation for Statistical Computing, Vienna, Austria. <https://www.R-project.org/> (2023).

Acknowledgements

This research was supported by CAL FIRE Forest Health Research grant 8GG21820; NASA Terrestrial Ecology Program – NASA GEDI Competed Science Team grant 80NSSC24K0571; NASA Earth Venture Program – GEDI Lidar: The Global Ecosystem Dynamics Investigation Lidar 80NSSC18K0338; and NASA Terrestrial Ecology Program – NASA GEDI Competed Science Team grant 80NSSC21K0189.

Author contributions

Christopher R. Hakkenberg: Funding acquisition, Conceptualization, Methodology, Resources, Software, Formal Analysis, Investigation, Writing – original draft, review and editing. Matthew L. Clark: Funding acquisition, Conceptualization, Methodology, Resources, Writing – review and editing. Tim Bailey: Writing – review and editing. Patrick Burns: Resources, Software, Writing – review and editing. Scott J. Goetz: Funding acquisition, Resources, Writing – review and editing.

Competing interests

The authors declare no competing interests.

Additional information

Supplementary information The online version contains Supplementary Material available at <https://doi.org/10.1038/s43247-024-01893-8>.

Correspondence and requests for materials should be addressed to Christopher R. Hakkenberg.

Peer review information *Communications Earth and Environment* thanks Victor Fernandez-Garcia and Bin Chen reviewers for their contribution to the peer review of this work. Primary Handling Editors: Alice Drinkwater and Mengjie Wang. A peer review file is available.

Reprints and permissions information is available at <http://www.nature.com/reprints>

Publisher's note Springer Nature remains neutral with regard to jurisdictional claims in published maps and institutional affiliations.

Open Access This article is licensed under a Creative Commons Attribution-NonCommercial-NoDerivatives 4.0 International License, which permits any non-commercial use, sharing, distribution and reproduction in any medium or format, as long as you give appropriate credit to the original author(s) and the source, provide a link to the Creative Commons licence, and indicate if you modified the licensed material. You do not have permission under this licence to share adapted material derived from this article or parts of it. The images or other third party material in this article are included in the article's Creative Commons licence, unless indicated otherwise in a credit line to the material. If material is not included in the article's Creative Commons licence and your intended use is not permitted by statutory regulation or exceeds the permitted use, you will need to obtain permission directly from the copyright holder. To view a copy of this licence, visit <http://creativecommons.org/licenses/by-nc-nd/4.0/>.

© The Author(s) 2024